



Research article

Genome-wide maps of nucleosomes of the trichostatin A treated and untreated archiascomycetous yeast *Saitoella complicata*

Kenta Yamauchi ¹, Shinji Kondo ², Makiko Hamamoto ³, Yutaka Suzuki ⁴,
and Hiromi Nishida ^{1,*}

¹ Biotechnology Research Center and Department of Biotechnology, Toyama Prefectural University, Imizu, Toyama 939-0398, Japan

² National Institute of Polar Research, Tokyo, Japan

³ Department of Life Sciences, School of Agriculture, Meiji University, Kanagawa, Japan

⁴ Department of Medical Genome Sciences, Graduate School of Frontier Sciences, University of Tokyo, Kashiwa, Japan

* **Correspondence:** E-mail: hnishida@pu-toyama.ac.jp; Tel: 81-766-56-7500;
Fax: 81-766-56-2498.

Abstract: We investigated the effects of trichostatin A (TSA) on gene expression and nucleosome position in the archiascomycetous yeast *Saitoella complicata*. The expression levels of 154 genes increased in a TSA-concentration-dependent manner, while the levels of 131 genes decreased. Conserved genes between *S. complicata* and *Schizosaccharomyces pombe* were more commonly TSA-concentration-dependent downregulated genes than upregulated genes. We calculated the correlation coefficients of nucleosome position profiles within 300 nucleotides (nt) upstream of a translational start of *S. complicata* grown in the absence and the presence of TSA (3 µg/mL). We found that 20 (13.0%) of the 154 TSA-concentration-dependent upregulated genes and 22 (16.8%) of the 131 downregulated genes had different profiles ($r < 0.4$) between TSA-free and TSA-treated. Additionally, 59 (38.3%) of the 154 upregulated genes and 58 (44.3%) of the 131 downregulated genes had similar profiles ($r > 0.8$). We did not observe a GC content bias between the 300 nt upstream of the translational start of the TSA-concentration-dependent genes with conserved nucleosome positioning and the genes with different nucleosome positioning, suggesting that TSA-induced nucleosome position change is likely not related to DNA sequence. Most gene promoters maintained their nucleosome positioning even after TSA treatment, which may be related to DNA sequence. Enriched and depleted dinucleotides distribution of *S. complicata* around the

midpoints of highly positioned nucleosome dyads was not similar to that of the phylogenetically close yeast *Schizosaccharomyces pombe* but similar to the basidiomycete *Mixia osmundae*, which has similar genomic GC content to that of *S. complicata*.

Keywords: archiascomycetes; histone acetylation; nucleosome position; *Saitoella complicata*; transcription; trichostatin A

1. Introduction

Eukaryotic genomic DNA is packaged with histones to form chromatin [1], the most fundamental repeating unit of which is the nucleosome [2]. The nucleosome consists of an octamer of histones, around which the DNA is wrapped 1.65 times [2]. Generally, histones are post-translationally modified [3]. Histone acetylation and deacetylation play important roles in the regulation of transcription [4,5]. Trichostatin A (TSA) is a histone deacetylase inhibitor, which induces hyperacetylation of histones [6,7].

Transcription (gene expression) and nucleosome position were compared between TSA-free and TSA-treated *Aspergillus fumigatus* (a member of the subphylum Pezizomycotina) [8]. Although TSA induced elongation of the nucleosomal DNA, most of the nucleosome positions were conserved in the gene promoters even after treatment with TSA [8].

The subphylum Taphrinomycotina (“Archiascomycetes”) is the earliest ascomycetous lineage during ascomycetous evolution [9,10]. The anamorphic and saprobic budding yeast *Saitoella complicata* is a member of Taphrinomycotina, which shares some characteristics with both ascomycetous and basidiomycetous yeasts [11]. Interestingly, the *S. complicata* genome is highly similar to Pezizomycotina genomes [12]. Although the fission yeast *Schizosaccharomyces pombe* also belongs to Taphrinomycotina, genomic characteristics are different between *S. complicata* and *Sch. pombe* [13]. In *Sch. pombe*, TSA alters the structural and functional imprint at the centromeres [14].

In this study, we investigate the effects of TSA on gene expression and nucleosome position in *S. complicata* and discuss the relationships between DNA sequence, gene expression, and nucleosome position. The genomic guanine-cytosine (GC) content of *S. complicata* (52.6%) is so different from that of *Sch. pombe* (36.1%). We elucidate whether the difference influences the nucleosome formation or not.

2. Methods

2.1. *Saitoella complicata* culturing

Saitoella complicata NBRC 10748 (= JCM 7358, = IAM 12963; type strain) was used in this study. The strain was cultivated in YM broth (yeast extract, 3 g/L; malt extract, 3 g/L; peptone, 5g/L; dextrose, 10 g/L) at 25 °C for 24 hours. *S. complicata* was cultured in the absence or the presence of TSA (1 µg/mL, 2 µg/mL, and 3 µg/mL).

2.2. Nucleosome mapping

S. complicata cultures grown in the presence of 0 µg/mL and 3 µg/mL TSA were used in the nucleosome mapping analysis. Equal volumes (22.5 mL) of *S. complicata* culture and 2% formaldehyde were mixed and incubated for 10 min followed by the addition of 5 mL of 1.25 M glycine. After *S. complicata* cells were collected and washed with 50 mM Tris-EDTA buffer (pH 8), the cells were suspended in zymolyase buffer (1 M sorbitol, 10 mM DTT, 50 mM Tris-HCl, pH 8.0). Zymolyase (Seikagaku corporation, Japan) (50 U) was added to the cell suspension and the solution was incubated at 37 °C for 1 h. The cells were collected by centrifugation and suspended in 2.5 mL of zymolyase buffer and MNase (Takara, Japan) (5 U) was added. The digestion reaction was incubated at 37 °C for 30 min and was stopped by adding sodium dodecylsulphate to a final concentration of 1% and ethylene diaminetetraacetic acid to a final concentration of 10 mM. Proteinase K solution (5 µg) was added to the solution and the mixture was incubated at 56 °C for 1 h. The solution was phenol/chloroform-extracted, ethanol-precipitated, and treated with RNase (Nippon Gene, Japan). Nucleosomal DNA fragments were isolated by electrophoresis using a 2% agarose gel. The mononucleosomal DNA band was excised and purified using the QIAquick Gel Extraction Kit (Qiagen). Both ends of the DNA fragments were sequenced using the Illumina HiSeq2500.

2.3. Mapping of nucleosome-mapping sequences

The read pairs were aligned to the genomic contigs (paired end 101 nucleotides (nt) and 150 nt insert) were mapped to the *S. complicata* genome [15] by using TopHat [16] and dereplicated by SAMtools [17]. Only uniquely mapped read pairs were used for the analysis. The DDBJ Supercomputer System [18] was used for mapping the Illumina reads to the genome and for additional analysis.

2.4. Overall disruption of nucleosome positioning in TSA-treated sample

To observe the trend of enrichment peaks, we operationally defined the peak positions of nucleosome dyads (dyad peaks) by using a threshold parameterization (the maximum pile (≥ 3) was given at the peak and in each of the ten up- and downstream positions flanking the peak; in seven or more position pairs the pile-level decreases outward from the peak).

2.5. Mapping of RNA-seq sequences and computation of expression levels

The RNAs were extracted and purified using the RNeasy Mini Kit (Qiagen). Quality of the extracted RNAs was checked by using Agilent 2100 Bioanalyzer. The Illumina sequences of single reads (36 nt length) were mapped to the *S. complicata* genome by using TopHat and dereplicated by SAMtools. The expression level of each gene (FPKM: fragments mapped per kilobase of transcript per million of mapped fragments) in the three samples was computed by using cuffdiff (<http://cole-trapnell-lab.github.io/cufflinks>) based on the coordinates mapped by the RNA-seq datasets.

2.6. Selection of genes with TSA-concentration-dependent expression

Based on the RNA expression data, we defined upregulated TSA-concentration-dependent genes as genes for which the expression level was at least 1.25 times higher when grown in 2 $\mu\text{g/mL}$ of TSA than when grown in 1 $\mu\text{g/mL}$ of TSA, and at least 1.25 times higher when grown in 3 $\mu\text{g/mL}$ of TSA than when grown in 2 $\mu\text{g/mL}$ of TSA. In addition, we defined downregulated TSA-concentration-dependent genes as genes for which the expression level was at least 0.75 times lower when grown in 2 $\mu\text{g/mL}$ of TSA than that of 1 $\mu\text{g/mL}$ of TSA, and that was at least 0.75 times lower when grown in 3 $\mu\text{g/mL}$ of TSA than that of 2 $\mu\text{g/mL}$ of TSA. Statistical estimation was performed by using edgeR [19].

3. Results

3.1. Characteristics of *S. complicata* cultured in 3 $\mu\text{g/mL}$ of TSA

We observed abnormal cell shape (inaccurate budding) of *S. complicata* when grown in 3 $\mu\text{g/mL}$ of TSA (Figure 1). Nucleosome formation is associated with the nucleosomal DNA sequence [20,21]. The dinucleotide sequence distributions were similar between TSA-free and TSA-treated, which were different from that of *Sch. pombe* (Figure 2).

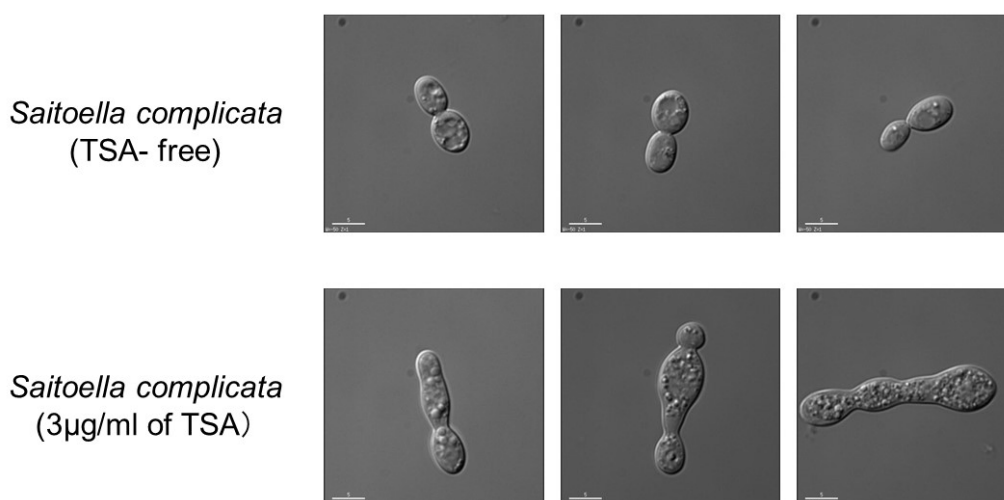


Figure 1. Micrographs of *Saitoella complicata*. *Saitoella complicata* was grown in YM broth (yeast extract, 3 g; malt extract, 3 g; peptone, 5g; dextrose, 10 g; water, 1 L) at 25 °C for 24 hours in 0 $\mu\text{g/mL}$ and 3 $\mu\text{g/mL}$ of TSA. The scale bar represents 5 μm .

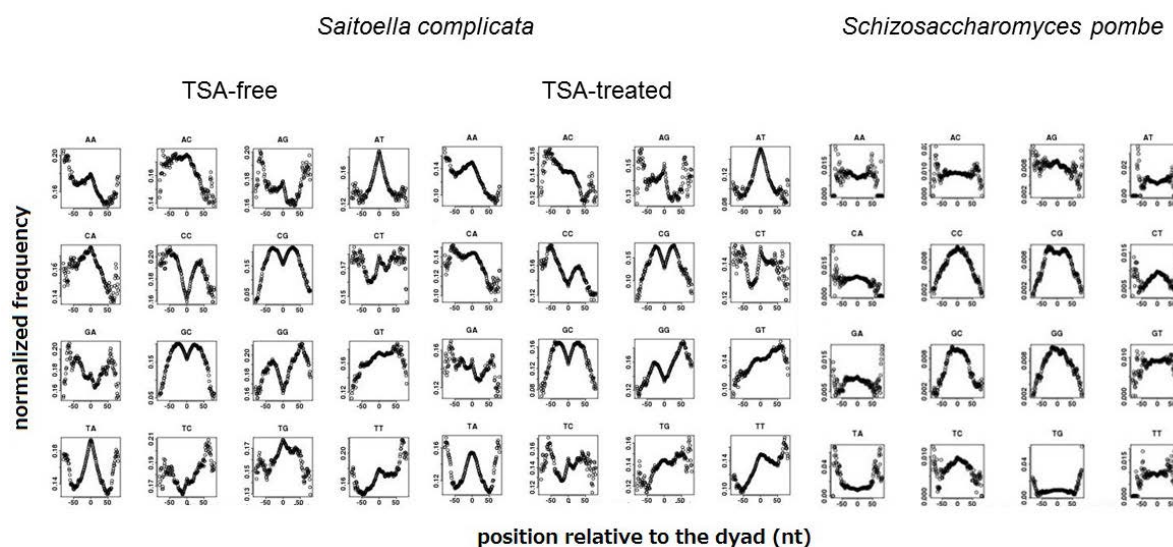


Figure 2. Enriched and depleted dinucleotides around the midpoints of highly positioned nucleosome dyads of TSA-free and TSA-treated *Saitoella complicata*, and *Schizosaccharomyces pombe*. The normalized frequencies of distances between highly positioned nucleosome dyads (5 or higher pile) and the closest dinucleotides are shown for TSA-free and TSA-treated samples. The frequencies are normalized to those found at all the genome positions. By using the dataset of wild-type cells of *Sch. pombe* [34], the distribution of distances to the closest dinucleotides around the dyads of highly positioned nucleosomes (3 or higher piles) the positions of the dyads of highly positioned nucleosomes (3 or higher piles) were computed. X- and y-axes represent distances to the closest dinucleotides from the dyad and normalized frequency of the closest dinucleotide found at the distance from the dyad.

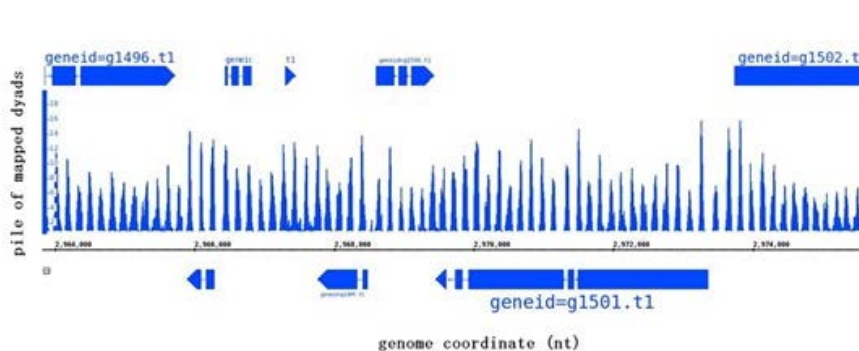


Figure 3. An example of pile levels of nucleosome dyads on the *Saitoella complicata* genome. The enrichment pattern shows ~150 nt spacing. The dyads are enriched around translation start sites (TSS), particularly downstream of genes.

We obtained 38872421 and 42603041 dereplicated sequence pairs for TSA-free and TSA-treated samples, respectively. Based on the genome positions mapped by paired sequences, we identified the dyads (mid-points) of nucleosomes. After counting the numbers of times mapped by the dyads (pile) [20] at each base on the genome, we computed average depth of mapped dyads

within ± 5 nts and used this average depth as the measure of nucleosome enrichment. A typical enrichment pattern of nucleosome dyads is shown in Figure 3.

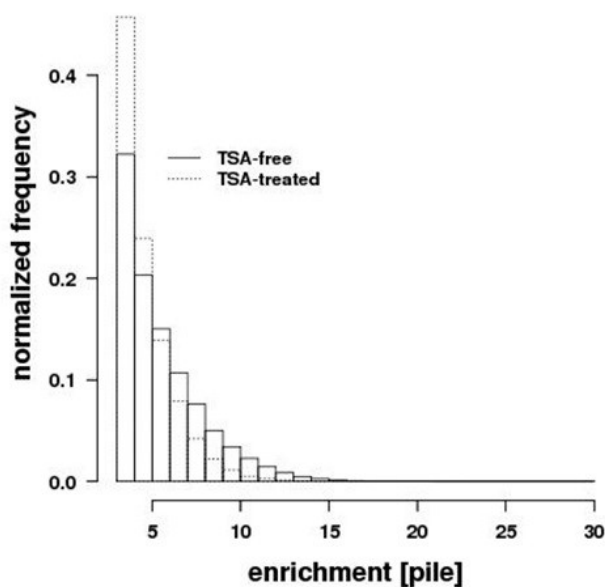


Figure 4. Overall level of positioning of nucleosome dyads. The numbers of nucleosome dyads of three or higher piles were compared between TSA-free and TSA-treated samples. The solid and dotted lines represent the distributions of TSA-free and TSA-treated samples, respectively.

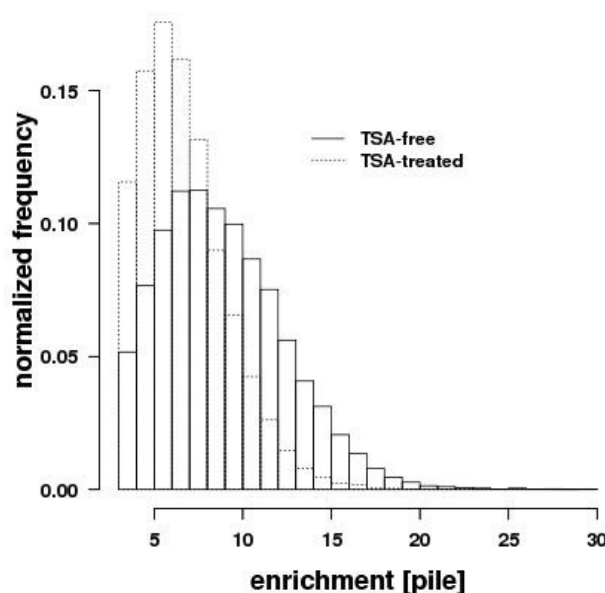


Figure 5. Overall level of positioning of peaks of nucleosome dyads. The numbers of peaks of nucleosome dyads of three or higher piles were compared between TSA-free and TSA-treated samples. The solid and dotted lines represent the distributions of TSA-free and TSA-treated samples, respectively.

We measured the overall level of nucleosome positioning by counting the number of highly positioned (piled) nucleosome dyads and compared it between the TSA-free and TSA-treated samples (Figure 4). The level of piles decreased significantly (Mann-Whitney U -test $p < 2.2 \times 10^{-16}$) in TSA-treated sample compared to TSA-free sample. We identified 26711 and 20704 dyad-peaks in the control and post-TSA samples, respectively. The disruption was more evident (Mann-Whitney U -test $p < 2.2 \times 10^{-16}$) when comparing the enrichment level of the dyad peaks as shown in Figure 5.

We obtained 68464078, 49183262, and 60631468 dereplicated sequences (pairs) for 1 $\mu\text{g/mL}$, 2 $\mu\text{g/mL}$ and 3 $\mu\text{g/mL}$ of TSA-treated samples, respectively.

The DNA sequences of the nucleosomal DNA fragments and cDNA fragments from transcribed RNA have been deposited in DDBJ under the accession number DRA003112 and DRA003113, respectively.

3.2. TSA-concentration-dependent up- and downregulated genes

The expression of 154 genes increased in a TSA-concentration-dependent manner (Table 1) while the expression of 131 genes decreased in a TSA-concentration-dependent manner (Table 2). For a total of 285 gene products, we searched for similar amino acid sequences to *Sch. pombe* proteins using BLASTP [22]. We found that 53 (34.4%) of the 154 TSA-concentration-dependent upregulated genes and 107 (81.7%) of the 131 downregulated genes have similar amino acid sequences to *Sch. pombe* proteins (Tables 1 and 2). Conserved genes between *S. complicata* and *Sch. pombe* were more commonly TSA-concentration-dependent downregulated genes. The gene ontology information about 53 of the 154 upregulated genes is shown in Supplementary Material 1, inferred from AmiGo version 1.8 (<http://amigo1.geneontology.org/cgi-bin/amigo/go.cgi>).

3.3. Conservation and variation of nucleosome position at promoter region

We compared the nucleosome position profiles within 500 nt upstream and downstream from a translational start (Supplementary Materials 2 and 3). We calculated the correlation coefficients of nucleosome position profiles within 300 nt upstream from a translational start of the samples grown in 0 $\mu\text{g/mL}$ and 3 $\mu\text{g/mL}$ of TSA (Tables 1 and 2). We found that 20 (13.0%) of the 154 TSA-concentration-dependent upregulated genes and 22 (16.8%) of the 131 downregulated genes had different profiles (Pearson product-moment correlation coefficient $r < 0.4$) between TSA-free and TSA-treated samples. Additionally, 59 (38.3%) of the 154 upregulated genes and 58 (44.3%) of the 131 downregulated genes had similar profiles ($r > 0.8$).

3.4. Guanine-cytosine (GC) content bias

We compared the GC content between the exons and introns in all the genes of *S. complicata*. The GC content in the exons (mean = 52.4%, SD = 5.81) was higher than that of the introns (mean = 48.0%, SD = 6.31) (Figure 4), which is consistent with previous reports [23–25].

Next, we compared the GC content of the 300 nt upstream of a translational start for the 20 upregulated and 22 downregulated genes with different nucleosome profiles and the 59 upregulated and 58 downregulated genes with similar nucleosome profiles. The result is shown in Figure 5. Based on the analysis of variance, there was no significant difference between the four samples.

4. Discussion

Enriched and depleted dinucleotides distributions around the midpoints of highly positioned nucleosome dyads were similar between TSA-free and TSA-treated samples (Figure 2), indicating that the relationship between histone proteins and DNA sequence is conserved. Interestingly, the distributions (especially, the dinucleotide sequences AT, CG, GC, and TA) are similar to those of the basidiomycete *Mixia osmundae* [26]. On the other hand, dinucleotide sequence distributions are different between *S. complicata* and *Sch. pombe*, except for CG and GC (Figure 2). Thus, the differences depended not on the phylogenetic relationships but on the genomic GC contents (*S. complicata*, 52.6 % of guanine-cytosine; *Sch. pombe*, 36.1%; and *M. osmundae*, 55.5%).

Of the 53 TSA-concentration-dependent upregulated genes with amino acid sequences similar to a *Sch. pombe* protein, we found the genes that were likely upregulated due to the addition of TSA (Supplementary Material 1). For example, the genes G7K_1405-t1, G7K_3794-t1, G7K_4487-t1, G7K_4488-t1, and G7K_4878-t1 encode transmembrane proteins that may play a role in TSA discharge. The genes G7K_1576-t1, G7K_2158-t2, G7K_3085-t1, G7K_3100-t1, G7K_3152-t1, G7K_3948-t1, G7K_4351-t1, G7K_4878-t1, and G7K_6152-t2 encode proteins related to cell cycle and replication and may play a role in cell division. The genes G7K_1912-t1, G7K_2003-t1, G7K_2534-t1, G7K_2954-t1, G7K_3743-t1, G7K_4481-t1, and G7K_5043-t1 encode proteins related to chromatin, telomere, and centromere maintenance and may play a role in repairing nucleosome structure and positioning (Supplementary Material 1).

In the filamentous ascomycetes *A. fumigatus* and *Aspergillus nidulans*, expression of the histone deacetylase coding gene *rpda* is stimulated by TSA [8,27]. *Schizosaccharomyces clr6* is similar gene to *Aspergillus rpda*. *S. complicata* has two similar genes (G7K_4324-t1 and G7K_6383-t1) to *clr6* [13]. However, the expression of these genes was not stimulated with TSA. Interestingly, in *S. complicata*, the histone methyltransferase coding gene *set2* homolog (G7K_4375-t1) expression increases in a TSA-concentration-dependent manner (Table 1), suggesting that the response of histone modification genes against TSA varies among ascomycetes.

Of the proteins that were encoded by the 107 TSA-concentration-dependent downregulated genes and that had amino acid sequences similar to that of *Sch. pombe*, most were essential for cell maintenance. This suggests that the cell metabolic activity of *S. complicata* decreases in a TSA-concentration-dependent manner.

Genome-wide comparative studies reveal that the GC content and nucleosome density tend to be higher in exons than in introns [23,28–32]. Nucleosome positioning is related to DNA sequence: regions rich in guanine and cytosine favor nucleosomes compared to regions rich in adenine and thymine [33]. In this study, we found that the GC content in the exons was higher than that in the introns (Figure 6). However, GC content bias was not observed between the 300 nt upstream of the translational start of the TSA-concentration-dependent genes with conserved nucleosome positioning and the genes with different nucleosome positioning (Figure 7). This result suggests that TSA-induced nucleosome position change is likely not related to DNA sequence. Most gene promoters maintain the nucleosome positioning even after TSA treatment, which may be related to DNA sequence.

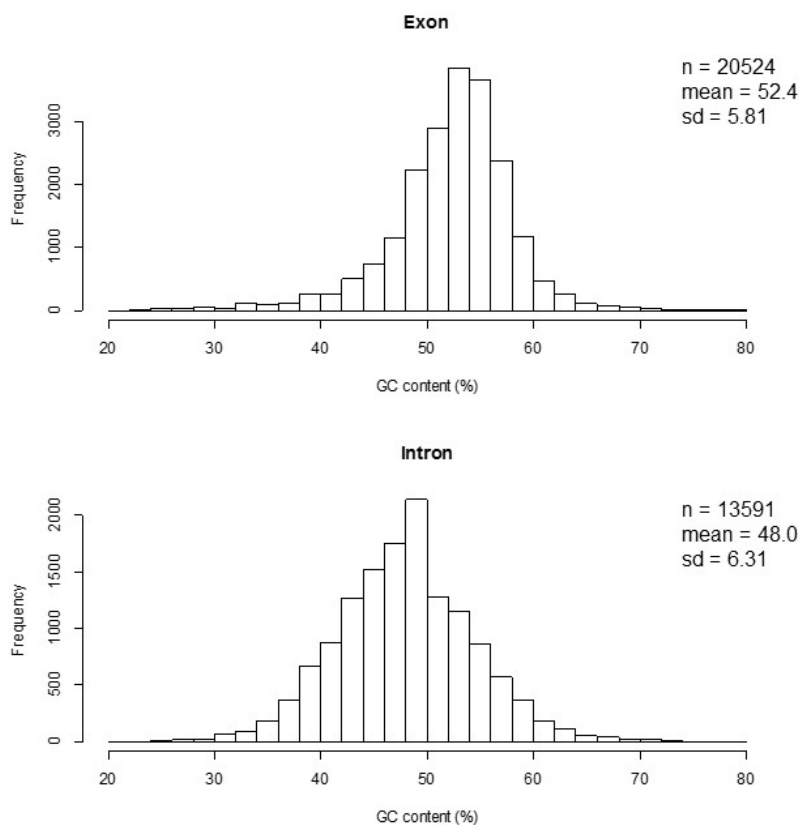


Figure 6. Histograms of GC content in exons and introns of *Saitoella complicata*. The number of exons and introns were 20524 and 13591, respectively.

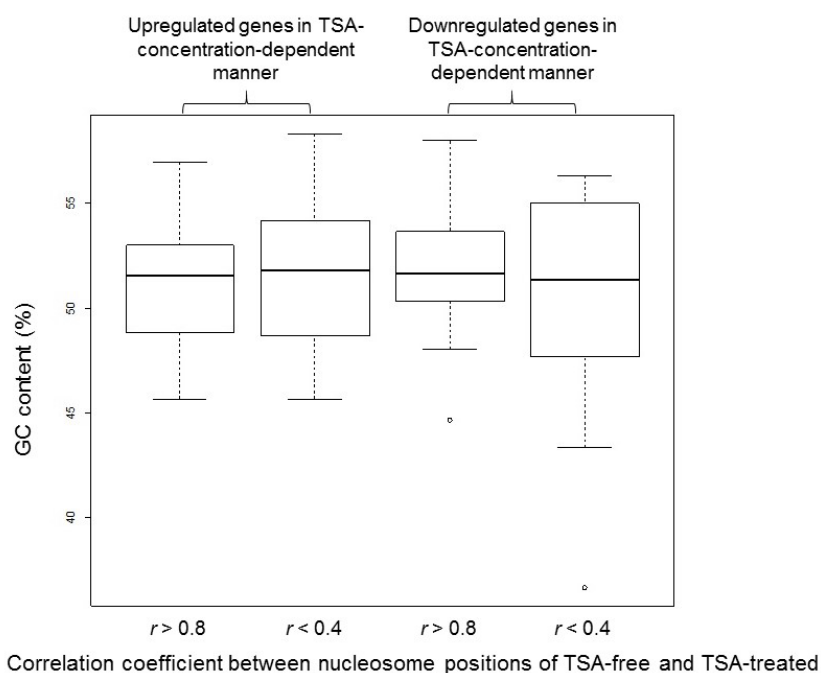


Figure 7. Boxplots of GC content of 300 nt upstream from a translational start of the 20 upregulated and 22 downregulated genes with different nucleosome profiles, and the 59 upregulated and 58 downregulated genes with similar nucleosome profiles.

We expected gene expression to be related to the amount of nucleosomes in a gene's promoter such that an increase of nucleosomes inhibits gene expression and a decrease activates expression. Among the 285 TSA-concentration-dependent genes, we found only nine candidate genes that fit this model (G7K_2954-t1, G7K_3456-t1, G7K_5145-t1, G7K_6368-t1, G7K_2158-t2, and G7K_4351-t1 of the 154 upregulated genes; G7K_2101-t1 and G7K6868-t1 of the 131 downregulated genes, Supplementary Materials 2 and 3). Therefore, in general, the amount and position of nucleosomes is maintained after TSA treatment.

5. Conclusion

In this study, we showed the nucleosome positioning robustness in the archiascomycetous yeast *Saitoella complicata*. Most gene promoters maintained their nucleosome positioning even after TSA treatment. Enriched and depleted dinucleotides distribution of *S. complicata* around the midpoints of highly positioned nucleosome dyads was not similar to that of the phylogenetically close yeast *Schizosaccharomyces pombe* but similar to the basidiomycete *Mixia osmundae*, which has similar genomic GC content to that of *S. complicata*.

Acknowledgment

This work was supported by JSPS KAKENHI grant no. 25440188 and 221S0002.

Conflict of Interest

The authors declare that there is no conflict of interest regarding the publication of this paper.

Table 1. Upregulated genes of *S. complicata* in TSA-concentration-dependent manner.

Locus tag (Protein ID)	Similar protein in <i>Schizosaccharomyces pombe</i>	E-value	Expression level in absence of TSA [13]	Expression level at 1 µg/mL TSA	Expression level at 2 µg/mL TSA	Expression level at 3 µg/mL TSA	Correlation coefficient of nucleosome position profiles between TSA-free and TSA-treated
G7K_0004-t1	no hit		6.7	22.7	29.6	37.2	0.93
G7K_0068-t1*#	gi_19114122_ref_NP_593210.1_DNA_endonuclease_III	0.056	51.3	134.3	256.8	338.2	0.86
G7K_0387-t2	no hit		10.8	25	39.2	53.6	0.87
G7K_0436-t1*	no hit		56.2	14.3	55	77.9	0.81
G7K_0451-t1	no hit		30.2	14	28.6	36	0.89
G7K_0476-t1*#	no hit		90.7	183	328.4	450.6	0.71
G7K_0489-t1	no hit		40.5	21.6	33.5	45.2	0.35
G7K_0499-t1*#	gi_429242433_ref_XP_004001772.1_histone-fold_domain-containing_protein	6×10^{-12}	460.8	299.3	540	751.4	0.11
G7K_0500-t1*	no hit		51.2	36.2	83.8	106	0.81
G7K_0501-t1*#	no hit		12.5	67.2	199.4	276.2	0.95
G7K_0518-t2	gi_429242230_ref_NP_593530.2_succinate_dehydrogenase_iron-sulfur_subunit_protein	2×10^{-28}	1.7	9.8	15	24.6	0.91
G7K_0720-t1*#	no hit		296.1	44.3	78.8	110.9	0.8
G7K_0856-t1	no hit		2.2	2.1	3.1	5.9	0.35
G7K_0936-t1	gi_19115704_ref_NP_594792.1_COP9_signalosome_complex_subunit_12_(predicted)	1×10^{-84}	68.5	2.2	2.9	4.4	0.79
G7K_0948-t1*	no hit		5.9	25.6	51.8	66.6	0.71
G7K_0986-t1	gi_295442985_ref_NP_593794.2_conserved_fungal_protein	4×10^{-30}	8.6	13.3	25.9	32.4	0.2
G7K_1025-t1	no hit		2.4	3.2	4.4	5.8	0.48
G7K_1096-t1	no hit		1.5	6	15.8	20.3	0.11
G7K_1111-t1	no hit		0.7	89	114.7	144.8	0.73
G7K_1196-t1	no hit		25.1	16.3	20.9	31.5	0.78

G7K_1237-t1*#	no hit		229.7	128.9	209.8	282	0.98
G7K_1324-t2	gi_19114225_ref_NP_593313.1_carboxylic_ester_hydrolase_activity_(predicted)	0.074	16.5	3.7	5.5	8.5	0.95
G7K_1389-t1	gi_19113165_ref_NP_596373.1_U6_snRNP-associated_protein_Lsm5_(predicted)	7×10^{-29}	3.7	11.4	19.1	28.1	0.81
G7K_1405-t1	gi_19113217_ref_NP_596425.1_hexose_transporter_Ght2	1×10^{-31}	57.4	15.8	23.7	29.7	0.78
G7K_1454-t1	gi_19114259_ref_NP_593347.1_retrotransposable_element	6×10^{-79}	1.8	0.3	1.1	1.3	0.88
G7K_1489-t1	no hit		36.8	17.1	21.6	28	0.78
G7K_1517-t2#	gi_19114517_ref_NP_593605.1_transcription_factor_(predicted)	1×10^{-21}	48.3	0.3	0.4	18.6	0.66
G7K_1553-t1#	no hit		88.5	218.7	318.7	400	0.64
G7K_1576-t1	gi_19113817_ref_NP_592905.1_glycerate_kinase_(predicted)	4×10^{-56}	59.2	18.5	29.3	36.8	0.96
G7K_1611-t1	no hit		1.6	0.2	0.3	0.7	0.94
G7K_1759-t1*	no hit		6.1	16.9	35.8	49.4	0.82
G7K_1847-t1#	gi_19111930_ref_NP_595138.1_oxysterol_binding_protein_(predicted)	2×10^{-116}	1.9	11.7	17.8	37.7	0.17
G7K_1862-t1*#	no hit		99.5	47.8	90.2	122.8	0.68
G7K_1912-t1	gi_19114445_ref_NP_593533.1_conserved_eukaryotic_protein	3×10^{-24}	13.4	17.4	30.3	38.5	0.9
G7K_1923-t1	no hit		92.9	16.6	25.2	31.5	0.6
G7K_1949-t1	no hit		2.4	3.3	7.2	9.2	0.62
G7K_1950-t1	no hit		1.3	0.4	0.7	1.5	0.79
G7K_1985-t1	gi_19112082_ref_NP_595290.1_ORMDL_family_protein_(predicted)	0.027	13.9	65.2	88	115.6	0.85
G7K_1992-t1	no hit		3.0	5.3	9.6	12.8	0.49
G7K_2003-t1	gi_19112851_ref_NP_596059.1_meiotic_cohesin_complex_subunit_Rec8	2×10^{-47}	23.6	48	62.5	82.7	0.84
G7K_2031-t1*	gi_19114220_ref_NP_593308.1_cyclophilin_family_peptidyl-prolyl_cis-trans_isomerase_Cyp1	5×10^{-78}	282.8	39.3	55.4	74.2	0.76
G7K_2060-t1	gi_19111966_ref_NP_595174.1_horsetail_movement_protein_Hrs1/Mcp6	0.048	9.5	19.3	36.1	46.4	0.65
G7K_2098-t1	gi_19115152_ref_NP_594240.1_WD_repeat_protein_Vps8_(predicted)	0.027	20.6	53.9	80.3	104.8	0.78
G7K_2107-t1#	no hit		17.1	100.7	148.8	206	0.81
G7K_2120-t2	gi_19114162_ref_NP_593250.1_CTNS_domain_protein_(SMART)	5×10^{-40}	83.8	12.8	17.3	21.9	0.95
G7K_2128-t1	gi_19113493_ref_NP_596701.1_hexaprenyldihydroxybenzoate_methyltransferase_(predicted)	8×10^{-28}	26.3	16	25.7	32.4	0.44
G7K_2158-t2#	gi_19113399_ref_NP_596607.1_DNA_replication_factor_C_complex_subunit_Rfc1	0	38.7	2.8	4.1	15.4	0.35
G7K_2199-t1*#	gi_162312510_ref_XP_001713094.1_dual_specificity_phosphatase_Stp1	3×10^{-58}	64.0	306.6	732	957.9	0.63
G7K_2200-t1*#	no hit		6.1	448.7	849.3	1116.9	0.63
G7K_2201-t1#	no hit		28.4	539.3	772.3	966.1	0.61

G7K_2230-t1	no hit		6.1	4.7	9.6	15.1	0.85
G7K_2285-t1	no hit		10.1	9.1	18	23.1	0.65
G7K_2286-t1	no hit		16.1	13.1	25.1	33.2	0.32
G7K_2288-t1*	no hit		19.0	18.2	37.7	47.5	0.83
G7K_2324-t1	no hit		71.8	39.4	53.2	72.9	0.89
G7K_2534-t1	gi_19114992_ref_NP_594080.1_chromatin_modification-related_protein	1×10^{-16}	86.5	30.1	45.7	57.7	0.92
G7K_2554-t1	no hit		4.2	8	16.3	21.6	0.76
G7K_2761-t1	no hit		0.0	0	0.1	6.4	0.58
G7K_2768-t1	no hit		75.7	12.2	17.5	25.5	-0.09
G7K_2894-t1	no hit		1.8	23.9	40.4	52.3	0.84
G7K_2896-t1	no hit		21.6	11.4	24.5	31.8	0.78
G7K_2953-t1*#	gi_429239757_ref_XP_004001700.1_DUF1242_family_protein_secretory_pathway_component_Ksh1_(predicted)	2×10^{-21}	285.9	201.2	349.5	445.6	0.81
G7K_2954-t1	gi_19115773_ref_NP_594861.1_ATP-dependent_DNA_helicase_Snf21	0.051	30.5	63.9	86.3	108.2	0.86
G7K_3085-t1	gi_19113352_ref_NP_596560.1_ATP-dependent_RNA_helicase_Slh1_(predicted)	6×10^{-94}	19.7	14	19.5	24.7	0.91
G7K_3100-t1	gi_19113146_ref_NP_596354.1_DNA_polymerase_epsilon_catalytic_subunit_Pol2	0.088	11.6	9	16.8	22	0.5
G7K_3101-t1	no hit		3.3	13	21.3	31.5	0.56
G7K_3126-t1	no hit		82.2	21.1	30	37.9	0.38
G7K_3141-t1	no hit		71.8	24.2	31.8	41.9	0.85
G7K_3152-t1	gi_63054647_ref_NP_594707.2_PPPDE_peptidase_family_(predicted)	7×10^{-25}	20.4	10.2	16.3	21	0.69
G7K_3172-t1	no hit		5.3	11.8	20.8	26.7	0.29
G7K_3369-t1	no hit		138.3	17.4	25.7	38.3	0.87
G7K_3412-t1	no hit		11.4	19.9	34.2	44.4	0.65
G7K_3434-t1	gi_429240854_ref_NP_596337.3_DUF55_family_protein	1×10^{-48}	82.2	31.8	41.9	57.3	0.54
G7K_3456-t1	gi_19114335_ref_NP_593423.1_anaphase-promoting_complex_subunit_Apc11	7×10^{-37}	65.7	43.2	57.8	73.8	0.21
G7K_3633-t1	no hit		10.4	17.3	33	42.8	0.75
G7K_3743-t1	gi_19075338_ref_NP_587838.1_nucleosome_assembly_protein_Nap1	0.095	43.1	26.9	39.2	52.8	0.95
G7K_3755-t1	no hit		4.6	3.2	4.2	5.3	0.82
G7K_3794-t1	gi_19114460_ref_NP_593548.1_membrane_transporter_(predicted)	1×10^{-92}	78.9	19.1	29.7	38.1	0.94
G7K_3802-t1	no hit		8.2	20.5	26.9	33.9	0.76
G7K_3825-t1	no hit		61.8	19.4	26.8	33.9	0.8

G7K_3854-t1	no hit		7.1	25.3	37.7	51.8	0.63
G7K_3935-t1	no hit		29.3	27	39.9	53.7	0.94
G7K_3948-t1	gi_19114683_ref_NP_593771.1_conserved_fungal_protein	2×10^{-42}	1.2	1.3	1.8	2.4	0.81
G7K_3958-t1	no hit		4.5	15.9	21	33.4	0.34
G7K_3981-t1	no hit		11.5	4.9	9.7	12.5	0.93
G7K_4023-t1	no hit		4.9	14.3	18	22.7	0.53
G7K_4104-t1	no hit		2.6	2.5	7.5	11.7	0.71
G7K_4107-t1	gi_19075830_ref_NP_588330.1_NADPH_quinone_oxidoreductase/ARE-binding_protein_(predicted)	6×10^{-30}	48.0	19.1	26.2	33.4	0.84
G7K_4228-t1	no hit		2.4	14.5	27.3	34.3	0.47
G7K_4279-t1	no hit		17.3	14.5	27.7	39	-0.04
G7K_4337-t1	no hit		12.8	8.8	16.5	21.6	0.57
G7K_4351-t1	gi_19075465_ref_NP_587965.1_sequence_orphan	0.04	53.1	62.7	79.1	100.5	0.74
G7K_4373-t1*#	gi_19115171_ref_NP_594259.1_cullin_1	0.061	92.2	231.6	493.6	624.5	0.79
G7K_4375-t1	gi_19115892_ref_NP_594980.1_histone_lysine_methyltransferase_Set2	5×10^{-30}	8.3	13.7	19.9	25	0.87
G7K_4481-t1	gi_19113570_ref_NP_596778.1_sister_chromatid_cohesion_protein/DNA_polymerase_eta_Eso1	7×10^{-112}	29.0	16.2	21.5	27.2	0.93
G7K_4487-t1	gi_19114232_ref_NP_593320.1_MFS_myo-inositol_transporter	2×10^{-35}	50.3	13.6	18.1	24.5	0.69
G7K_4488-t1	gi_19113098_ref_NP_596306.1_membrane_transporter_(predicted)	3×10^{-4}	12.3	14.5	21.9	27.6	0.76
G7K_4531-t1	gi_19114945_ref_NP_594033.1_vacuolar_carboxypeptidase_(predicted)	1×10^{-108}	10.7	11.5	18.9	24.3	0.65
G7K_4562-t1*#	no hit		20.1	115.9	206.7	263	0.51
G7K_4621-t1	no hit		90.0	50.2	73.5	96.8	0.43
G7K_4626-t1*	no hit		3.0	9.4	21.6	33.7	0.88
G7K_4723-t1#	no hit		200.4	216.3	300.9	423.3	0.55
G7K_4758-t2	no hit		155.8	21.7	27.8	38.5	0.83
G7K_4872-t1#	no hit		1.4	30.4	51.3	80.1	0.8
G7K_4878-t1	gi_19114272_ref_NP_593360.1_acetate_transmembrane_transporter_(predicted)	1×10^{-19}	129.0	11.2	14.2	18.8	0.89
G7K_4889-t1*	no hit		13.2	40.7	93.8	117.6	0.54
G7K_4910-t1	no hit		17.2	24.2	36.1	45.7	0.88
G7K_5043-t1	gi_19113028_ref_NP_596236.1_cryptic_loci_regulator_Clr1	0.037	3.6	13.9	19.1	24.3	0.82
G7K_5072-t1*#	no hit		6.9	183.9	351.3	477.6	0.54
G7K_5145-t1	no hit		5.5	5.5	9.8	12.7	0.52

G7K_5191-t1	no hit		5.7	10.6	22.9	30.7	0.59
G7K_5192-t1	no hit		0.0	14.4	23.4	29.5	0.92
G7K_5194-t1	no hit		1234.1	41.8	57.8	73	0.94
G7K_5234-t1	no hit		7.5	9.6	19	24.2	-0.06
G7K_5242-t1	no hit		63.8	12.8	18	22.6	0.76
G7K_5356-t2	no hit		57.4	11.6	17.2	21.6	0.75
G7K_5404-t1	no hit		5.5	5.6	10.4	14.7	0.58
G7K_5504-t1	gi_19113988_ref_NP_593076.1_S-methyl-5-thioadenosine_phosphorylase_(predicted)	0.022	1.8	1.8	3.5	5.1	0.59
G7K_5505-t1	no hit		0.8	2.1	2.9	3.8	0.71
G7K_5583-t1	no hit		15.6	11.4	18.6	23.9	0.29
G7K_5604-t1	no hit		14.6	14.5	19.2	25.4	0.77
G7K_5676-t1	no hit		12.2	11.1	17.1	23.4	-0.02
G7K_5680-t1	no hit		15.8	12.4	26.4	34.1	0.52
G7K_5760-t1	no hit		25.3	15.5	21.1	26.9	0.9
G7K_5784-t1	no hit		1.1	0.4	0.8	1.1	0.63
G7K_5886-t1	no hit		12.2	52.5	79.2	102	0.74
G7K_6048-t1	gi_19113866_ref_NP_592954.1_ribosome_biogenesis_protein_(predicted)	5×10^{-10}	159.6	59.4	85.1	111	0.67
G7K_6074-t1	no hit		12.2	19.2	27.4	34.4	0.71
G7K_6151-t1	no hit		1.3	6.9	12.7	21.6	0.63
G7K_6152-t2*	gi_19115599_ref_NP_594687.1_histidine_kinase_Mak1	8×10^{-15}	7.2	0	6.1	16.1	0.93
G7K_6188-t1	no hit		0.6	0.9	2.4	3.1	0.9
G7K_6280-t1*	no hit		5.9	50.3	95.2	124.2	0.77
G7K_6291-t1	no hit		5.2	13.5	19.1	24.3	0.57
G7K_6301-t2	gi_19115307_ref_NP_594395.1_sequence_orphan	1×10^{-10}	26.6	0	0	0	0.54
G7K_6361-t1	gi_19075350_ref_NP_587850.1_60S_ribosomal_protein_L36	3×10^{-14}	2335.0	1	1.9	3.3	0.37
G7K_6443-t1	no hit		16.9	20.9	34.5	46.2	0.82
G7K_6445-t1	gi_19114696_ref_NP_593784.1_nonsense-mediated_decay_protein_Upf2	0.04	9.2	13.8	19.9	28.9	0.95
G7K_6454-t1	gi_429239609_ref_NP_595180.2_branched_chain_amino_acid_aminotransferase_Eca39	4×10^{-105}	148.9	21.7	29.6	38.5	0.57
G7K_6461-t1	no hit		9.4	20.5	30.7	40.6	0.85
G7K_6499-t1	no hit		2.2	2.7	5	6.3	0.55

G7K_6500-t1	gi_19114259_ref_NP_593347.1_retrotransposable_element	9×10^{-17}	1.2	1.1	2.1	4.2	0.11
G7K_6510-t1	no hit		10.1	17.8	23.2	30.7	0.75
G7K_6529-t1	no hit		23.2	20	27.7	34.7	0.89
G7K_6553-t1*#	no hit		62.6	56.1	95.3	131.9	0.48
G7K_6600-t1	no hit		194.5	27.9	36.7	46.3	0.27
G7K_6735-t1	no hit		48.7	27.9	48.3	64.6	0.86
G7K_6744-t1	no hit		8.8	34.9	50	71	0.72
G7K_6763-t1	no hit		3.3	2.7	5.2	9.3	0.65
G7K_6768-t1	gi_19114326_ref_NP_593414.1_nucleoporin_Nup184	0.022	25.3	7.6	9.8	12.3	0.47
G7K_6770-t1	no hit		5.9	48.3	62	84.2	0.89
G7K_6829-t1	gi_19114998_ref_NP_594086.1_transcriptional_repressor_Sak1	3×10^{-68}	30.5	7.1	9	12.7	0.88
G7K_6872-t1	no hit		6.3	7.9	10.1	13.1	NA
G7K_6887-t1	no hit		76.9	34	47.7	62.2	0.92
G7K_6914-t1	no hit		19.3	19	30.2	42.4	0.89

*Significantly ($p < 0.05$) differentially expressed genes between growths in 1 $\mu\text{g/mL}$ and 2 $\mu\text{g/mL}$ of TSA.

#Significantly ($p < 0.05$) differentially expressed genes between growths in 2 $\mu\text{g/mL}$ and 3 $\mu\text{g/mL}$ of TSA.

Table 2. Downregulated genes of *S. complicata* in TSA-concentration-dependent manner.

Locus tag (Protein ID)	Similar protein in <i>Schizosaccharomyces pombe</i>	E-value	Expression level in absence of TSA [13]	Expression level at 1 µg/mL TSA	Expression level at 2 µg/mL TSA	Expression level at 3 µg/mL TSA	Correlation coefficient of nucleosome position profiles between TSA-free and TSA-treated
G7K_0147-t1*#	gi_19075316_ref_NP_587816.1_malate_dehydrogenase_(predicted)	3×10 ⁻¹¹⁴	576.9	204.3	132.8	94	0.34
G7K_0202-t1*#	gi_19114075_ref_NP_593163.1_superoxide_dismutase_Sod1	9×10 ⁻⁷⁴	1713.3	2241.2	1114.7	780.8	0.14
G7K_0215-t1#	gi_19115831_ref_NP_594919.1_F1-ATPase_alpha_subunit	0	351.0	1288.4	957.9	670.4	0.94
G7K_0234-t1*#	gi_19113755_ref_NP_592843.1_MAP_kinase_Sty1	0	283.9	326	192	137.9	0.91
G7K_0252-t1*#	gi_162312257_ref_NP_596103.2_2-isopropylmalate_synthase_Leu3	0	98.1	256.6	149.9	109.3	0.51
G7K_0263-t1*#	gi_19114714_ref_NP_593802.1_mitochondrial_hydrogen/potassium_transport_system_protein_(predicted)	1×10 ⁻¹⁹	215.4	281	161.1	108.7	0.78
G7K_0549-t1#	gi_19075198_ref_NP_587698.1_ubiquinol-cytochrome-c_reductase_complex_core_protein_Qcr2_(predicted)	2×10 ⁻⁶⁹	103.1	245.3	180.6	131	0.87
G7K_0595-t1*#	gi_429242423_ref_NP_593718.2_citrate_synthase_Cit1	0	602.7	1031.8	710.8	482.6	0.77
G7K_0632-t1*#	gi_19075303_ref_NP_587803.1_19S_proteasome_regulatory_subunit_Rpn8_(predicted)	1×10 ⁻¹⁴²	181.0	294.6	186.8	132.4	0.77
G7K_0674-t1*#	gi_19113610_ref_NP_596818.1_tetra_spanning_protein_1_Tts1	4×10 ⁻³⁰	482.8	670	406.3	282.4	0.94
G7K_0679-t1#	gi_19075785_ref_NP_588285.1_translation_elongation_factor_eEF3	0	312.0	712.7	525.1	382.1	0.48
G7K_0762-t1*#	gi_19112660_ref_NP_595868.1_NADH-dependent_flavin_oxidoreductase_(predicted)	3×10 ⁻¹⁰⁰	218.5	356.7	217.8	147.7	-0.05
G7K_0764-t1*#	gi_429239441_ref_NP_588570.2_cell_surface_glycoprotein_(predicted),_DUF1773_family_protein_4	0.017	868.7	483.9	265.2	166.6	0.85
G7K_0808-t1#	gi_19115677_ref_NP_594765.1_cell_wall_protein_Gas1,_1,3-beta-glucanosyltransferase_(predicted)	2×10 ⁻¹⁶¹	310.1	275.2	202.3	150.6	0.96
G7K_1000-t1*#	gi_19075182_ref_NP_587682.1_catalase	2×10 ⁻¹⁰²	668.0	643.7	419.8	279.1	0.3
G7K_1215-t1*#	gi_19075725_ref_NP_588225.1_translation_release_factor_class_II_eRF3	0	177.9	181.4	110.8	80.1	0.86
G7K_1218-t1*#	gi_162312364_ref_XP_001713040.1_20S_proteasome_component_alpha_3_(predicted)	8×10 ⁻¹⁰⁸	448.8	408.7	213.3	144.9	0.87
G7K_1248-t1*#	gi_19112638_ref_NP_595846.1_cytochrome_c1_Cyt1_(predicted)	7×10 ⁻¹²⁷	8.1	344.7	234.7	161.2	0.04
G7K_1281-t1*#	gi_19113828_ref_NP_592916.1_20S_proteasome_component_beta_4_(predicted)	6×10 ⁻⁸⁹	366.9	376.7	211.4	151.8	0.76
G7K_1323-t1#	gi_19075527_ref_NP_588027.1_IMP_cyclohydrolase/phosphoribosylaminoimidazolecarboxamideformyltransferase	0	187.3	234.3	164.6	116	0.94
G7K_1362-t1*#	gi_19075540_ref_NP_588040.1_20S_proteasome_component_alpha_7_Pre10_(predicted)	3×10 ⁻⁶⁰	326.0	572.1	337.2	238.9	0.64

G7K_1363-t1*#	no hit		335.9	631.3	325.9	233.5	0.61
G7K_1496-t1#	gi_19075670_ref_NP_588170.1_acyl-coA_desaturase_(predicted)	0	452.7	278.8	192.1	142.2	0.94
G7K_1561-t1*#	gi_19115284_ref_NP_594372.1_20S_proteasome_component_alpha_5_Pup2_(predicted)	5×10^{137}	285.3	368.5	190.6	124.9	0.8
G7K_1595-t1*#	gi_19112272_ref_NP_595480.1_19S_proteasome_regulatory_subunit_Rpt2	0	166.0	389	248	186	0.87
G7K_1606-t1*	gi_19114341_ref_NP_593429.1_UBX_domain_protein_Ubx3_Cdc48_cofactor	3×10^{61}	210.7	158.2	89.4	65.7	0.95
G7K_1630-t1#	gi_19113237_ref_NP_596445.1_mannose-6-phosphate_isomerase_(predicted)	4×10^{91}	137.7	95.8	60.2	36.8	0.94
G7K_1663-t1*#	gi_19114753_ref_NP_593841.1_phosphoric_monoester_hydrolase_(predicted)	6×10^{58}	513.2	294.3	181.5	130.5	0.92
G7K_1703-t1#	no hit		111.5	298.5	221.4	164.3	0.85
G7K_1750-t1#	gi_19114508_ref_NP_593596.1_sequence_orphan	0.076	640.9	429.5	298.7	188	0.83
G7K_1847-t2#	gi_19111930_ref_NP_595138.1_oxysterol_binding_protein_(predicted)	6×10^{115}	669.3	162	115.3	73.6	0.17
G7K_1885-t1*#	gi_19112945_ref_NP_596153.1_phosphoglucomutase_(predicted)	0	333.4	303.2	189.6	136.4	0.78
G7K_1886-t1#	gi_19112660_ref_NP_595868.1_NADH-dependent_flavin_oxidoreductase_(predicted)	1×10^{150}	124.0	195.4	140.5	102.9	0.48
G7K_1891-t1#	gi_19112484_ref_NP_595692.1_fructose-bisphosphate_aldolase_Fba1	3×10^{176}	422.8	805.9	590.3	404.8	0.89
G7K_1908-t1*#	gi_19113003_ref_NP_596211.1_NAD_dependent_epimerase/dehydratase_family_protein	3×10^{13}	261.6	235.8	158.7	118.2	0.82
G7K_1940-t1*	gi_19112174_ref_NP_595382.1_acetolactate_synthase_catalytic_subunit	0	195.1	143.2	84.7	62.7	0.74
G7K_2008-t1#	gi_295442792_ref_NP_588397.3_fumarate_hydratase_(predicted)	0	587.3	846.2	617.3	415.1	0.85
G7K_2064-t1*#	no hit		2067.0	408.5	229.3	167.9	0.53
G7K_2069-t1*#	gi_19114777_ref_NP_593865.1_hexokinase_2	2×10^{123}	269.4	441.1	271.9	181.6	0.97
G7K_2101-t1*#	gi_19114158_ref_NP_593246.1_ATP-citrate_synthase_subunit_2_(predicted)	0	367.8	293.2	151.9	101.8	0.56
G7K_2323-t1*#	gi_19112075_ref_NP_595283.1_ubiquitin_conjugating_enzyme_Ubc4	7×10^{70}	1514.7	479.5	294.8	204.1	0.83
G7K_2351-t1*#	gi_63054710_ref_NP_595282.2_19S_proteasome_regulatory_subunit_Rpn3	1×10^{159}	196.7	207.2	92.3	60.5	0.82
G7K_2360-t1#	gi_19113123_ref_NP_596331.1_dihydrolipoyllysine-residue_succinyltransferase	2×10^{168}	673.0	139.8	92.3	65.9	0.94
G7K_2374-t1*#	gi_19113114_ref_NP_596322.1_mitochondrial_Mam33_family_protein_(predicted)	1×10^{28}	378.7	660.1	404.3	273.6	0.81
G7K_2426-t1#	gi_19113109_ref_NP_596317.1_serine/threonine_protein_phosphatase_PP1	0	260.1	291.8	213.5	153.6	0.85
G7K_2476-t1*	no hit		144.8	88.8	53.2	36.9	0.9
G7K_2810-t1*#	gi_19115013_ref_NP_594101.1_20S_proteasome_component_alpha_6_subunit_Pre5_(predicted)	5×10^{103}	267.4	172.6	90.4	64.1	-0.07
G7K_2811-t1*#	no hit		2855.1	1196.1	690.2	497.1	-0.1
G7K_3019-t1#	gi_19075363_ref_NP_587863.1_translation_elongation_factor_2_(EF-2)_Eft2,B	0	627.0	1586.5	1160.9	814.6	0.91
G7K_3069-t1*#	no hit		264.5	196.5	116.4	87	0.63
G7K_3139-t1*#	gi_19075931_ref_NP_588431.1_BAX_inhibitor_family_protein_Bxi1	1×10^{08}	561.2	528.8	308.8	223.1	0.71

G7K_3223-t2*#	gi_19112979_ref_NP_596187.1_40S_ribosomal_protein_S23	1×10^{-73}	206.7	474.8	294.2	201.5	0.7
G7K_3234-t1#	gi_19112083_ref_NP_595291.1_asparagine_synthetase	0	134.2	285.2	210.5	153.3	0.94
G7K_3235-t1*#	no hit		360.6	993.7	568.3	365.4	0.19
G7K_3283-t1*#	gi_19111957_ref_NP_595165.1_20S_proteasome_component_alpha_4_Pre6	1×10^{-122}	146.4	305.2	168.4	117.2	0.86
G7K_3385-t1*#	gi_19114337_ref_NP_593425.1_V-type_ATPase_V1_domain_subunit_A	0	397.8	149.1	79.1	43.2	0.91
G7K_3396-t2	gi_19115251_ref_NP_594339.1_glucan_1,4-alpha-glucosidase_(predicted)	0	50.5	7.7	4.7	2.9	0.57
G7K_3517-t1*#	gi_19113523_ref_NP_596731.1_S-adenosylmethionine_synthetase	0	170.0	1240.7	659.9	432.3	0.83
G7K_3576-t1*#	gi_19112963_ref_NP_596171.1_19S_proteasome_regulatory_subunit_Mts4	0	152.5	254.5	139.2	95.1	0.76
G7K_3638-t1*#	no hit		1819.6	572.8	381.5	271.8	0.66
G7K_3645-t1*#	no hit		218.7	891.1	586.7	392.2	0.77
G7K_3680-t1*#	gi_19114264_ref_NP_593352.1_homocysteine_methyltransferase_Met26	4×10^{-10}	61.8	249.8	127.1	82.1	0.03
G7K_3703-t1*#	no hit		369.9	196.8	123.2	83.9	0.86
G7K_3714-t1*	gi_295442859_ref_NP_595976.2_topoisomerase_II-associated_deadenylation-dependent_mRNA-decapping_factor_(predicted)	1×10^{-123}	80.0	90.3	54.2	40	0.54
G7K_3737-t1*#	gi_19114527_ref_NP_593615.1_ubiquitinated_histone-like_protein_Uhp1	4×10^{-80}	257.3	662.9	391.6	292	0.82
G7K_3769-t1	gi_429238683_ref_NP_587854.2_kinetochore_protein_Mis18	8×10^{-24}	114.2	89.5	61.2	42.5	0.2
G7K_3850-t1	gi_19075178_ref_NP_587678.1_ThiJ_domain_protein	2×10^{-11}	1003.1	120	80.3	59.2	0.87
G7K_3853-t1#	gi_19113860_ref_NP_592948.1_hexokinase_1	1×10^{-171}	50.8	121.1	90.3	48.6	0.74
G7K_3870-t1*#	gi_19115456_ref_NP_594544.1_20S_proteasome_component_beta_2_(predicted)	1×10^{-123}	393.4	309.4	170.5	116.4	0.87
G7K_3892-t1*#	gi_19112166_ref_NP_595374.1_20S_proteasome_component_alpha_1_(predicted)	1×10^{-76}	291.4	278	168.9	126.2	0.82
G7K_3929-t1*#	gi_19112028_ref_NP_595236.1_glyceraldehyde_3-phosphate_dehydrogenase_Gpd3	1×10^{-177}	336.0	2659.7	1856.3	1288.9	0.65
G7K_3952-t1*#	gi_19112883_ref_NP_596091.1_heat_shock_protein_Hsp16	5×10^{-7}	767.7	419.2	220.8	156.5	0.71
G7K_3969-t1*#	gi_19114312_ref_NP_593400.1_glutamate-ammonia_ligase_Gln1	0	1245.3	882	619	442.4	0.76
G7K_3976-t1	gi_19112179_ref_NP_595387.1_ADP-ribose_diphosphatase_NudF_subfamily_(predicted)	2×10^{-75}	262.4	79.9	51.8	37.2	0.66
G7K_3978-t1#	gi_19115256_ref_NP_594344.1_3-hydroxyacyl-CoA_dehydrogenase_(predicted)	3×10^{-83}	427.8	173	115.5	79.6	0.58
G7K_4017-t1#	no hit		717.8	1128.8	805.4	560.6	0.87
G7K_4024-t1*#	gi_429238993_ref_NP_588144.2_prohibitin_Phb2_(predicted)	3×10^{-139}	971.2	626	360.8	242.3	0.61
G7K_4029-t1#	gi_19075641_ref_NP_588141.1_phosphoribosylaminoimidazole_carboxylase_Ade6	0	66.5	149.5	110.9	79.2	0.88
G7K_4074-t1#	no hit		2060.7	972.6	714.4	512.5	0.92
G7K_4151-t1*#	gi_63054529_ref_NP_593287.2_AAA_family_ATPase_Cdc48	0	269.5	310.5	169.4	122.6	0.93
G7K_4199-t1#	gi_19115300_ref_NP_594388.1_5-aminolevulinate_synthase_(predicted)	0	157.2	149.7	104.6	77.2	0.39

G7K_4282-t1*#	gi_19112456_ref_NP_595664.1_cyclophilin_family_peptidyl-prolyl_cis-trans_isomerase_Cyp2	1×10 ⁹⁹	1439.1	2241.3	1518.3	988.8	0.73
G7K_4306-t1*#	gi_19113838_ref_NP_592926.1_WD_repeat-containing_protein	0.032	400.9	397.4	266.6	188.6	0.72
G7K_4365-t1*#	gi_19075632_ref_NP_588132.1_UTP-glucose-1-phosphate_uridylyltransferase_(predicted)	8×10 ⁻³⁶	547.8	723.8	414.9	269.1	0.73
G7K_4366-t1*#	no hit		638.8	951.5	579.5	416.4	0.9
G7K_4517-t1#	gi_19112201_ref_NP_595409.1_ubiquitin	2×10 ⁻¹⁰¹	508.6	648.5	469.7	335.5	-0.25
G7K_4556-t1*#	gi_19113238_ref_NP_596446.1_beta-glucosidase_Psu2_(predicted)	4×10 ⁻¹⁰⁷	261.7	295.2	168.4	97.3	0.38
G7K_4642-t1*#	gi_19115123_ref_NP_594211.1_mitochondrial_2-oxoadipate_and_2-oxoglutarate_transporter_(predicted)	4×10 ⁻¹²⁷	198.6	172	112.5	82.9	0.79
G7K_4647-t1*#	gi_19115142_ref_NP_594230.1_succinate-CoA_ligase_alpha_subunit_(predicted)	5×10 ⁻¹⁵⁵	504.6	454.4	282.9	200.7	0.86
G7K_4662-t1*#	gi_19112410_ref_NP_595618.1_actin_Act1	0	824.1	1039.1	658	423.1	0.61
G7K_4696-t1*#	gi_19114023_ref_NP_593111.1_19S_proteasome_regulatory_subunit_Rpn6_(predicted)	1×10 ⁻¹⁵⁵	174.6	275.8	165.2	117.1	0.85
G7K_4699-t1*#	gi_19112359_ref_NP_595567.1_histone_H3_h3.2	2×10 ⁻⁹¹	1774.9	1032.7	673.3	484.4	0.4
G7K_4745-t1	gi_19115641_ref_NP_594729.1_20S_proteasome_component_beta_6	3×10 ⁻³¹	336.3	91.3	59.3	43	0.29
G7K_4813-t1*#	gi_19114136_ref_NP_593224.1_methylenetetrahydrofolate_reductase_Met9	0	90.8	191	107	79.5	0.9
G7K_4847-t1#	gi_19114548_ref_NP_593636.1_inorganic_pyrophosphatase_(predicted)	5×10 ⁻¹⁵⁵	586.6	1273.7	936.3	650.6	0.83
G7K_4869-t1*#	gi_19111913_ref_NP_595121.1_alcohol_dehydrogenase_(predicted)	5×10 ⁻¹⁰⁴	114.9	306.5	135.6	81	0.75
G7K_4938-t1*#	gi_162312184_ref_NP_595526.2_transmembrane_receptor_Wsc1_(predicted)	2×10 ⁻¹⁵	658.3	423.1	283.1	204.6	0.91
G7K_4969-t1#	gi_19115804_ref_NP_594892.1_pyruvate_dehydrogenase_e1_component_alpha_subunit_Pda1_(predicted)	0	390.8	324	223.8	152	0.91
G7K_5057-t1*#	gi_162312305_ref_XP_001713148.1_ubiquitin_activating_enzyme_E1	0	298.9	214.3	114.6	84.1	0.86
G7K_5063-t1*#	no hit		1403.2	188.4	108.1	76.9	0.62
G7K_5162-t1	gi_19113624_ref_NP_596832.1_UDP-N-acetylglucosamine_diphosphorylase_Uap1/Qri1(predicted)	1×10 ⁻¹¹⁵	132.3	118.7	79.1	59	0.62
G7K_5321-t1*#	gi_19115722_ref_NP_594810.1_pyridoxamine_5'-phosphate_oxidase_(predicted)	4×10 ⁻⁵²	504.7	228.8	149	107.7	0.46
G7K_5384-t1*	no hit		188.7	113.6	69.9	52.3	0.68
G7K_5501-t1#	no hit		1.8	99.8	71.6	49	0.71
G7K_5530-t1*#	gi_19111898_ref_NP_595106.1_tubulin_alpha_2	0	556.2	639.1	446.1	325.9	0.84
G7K_5545-t1*#	gi_68013174_ref_NP_001018848.1_thioredoxin_reductase_Trr1	7×10 ⁻¹⁶⁶	44.8	171.9	95.2	65.7	0.91
G7K_5751-t1#	gi_19112381_ref_NP_595589.1_mitochondrial_glutathione_reductase_Pgr1	0	113.3	155.4	101.8	65.9	0.94
G7K_5848-t1	gi_19115217_ref_NP_594305.1_thymidylate_synthase_(predicted)	2×10 ⁻⁶⁵	76.3	82.9	55.3	40.4	0.84
G7K_5853-t1#	no hit		300.8	194.5	140.3	101.5	0.36
G7K_5962-t1	no hit		28.3	59.9	44.9	33.2	0.37
G7K_5982-t1*#	gi_19075803_ref_NP_588303.1_translation_elongation_factor_EF-1_beta_subunit_(eEF1B)	2×10 ⁻⁷²	287.4	1561.8	1016.6	729.1	0.93

G7K_6002-t1*#	no hit		288.3	240.2	123.8	76.8	0.3
G7K_6163-t1*#	gi_19114506_ref_NP_593594.1_19S_proteasome_regulatory_subunit_Rpn9	3×10 ⁻¹²⁷	134.1	180.2	96.7	65.8	0.81
G7K_6170-t1#	gi_19114408_ref_NP_593496.1_dihydrolipoamide_dehydrogenase_Dld1	0	282.9	296.2	218.5	161	0.67
G7K_6181-t1*#	no hit		310.3	2072.9	1436.1	997.6	0.35
G7K_6190-t1*	gi_19111859_ref_NP_595067.1_isocitrate_lyase_(predicted)	3×10 ⁻¹⁰⁷	862.5	79.9	37.2	27.2	0.58
G7K_6245-t1	gi_63054449_ref_NP_588301.2_Swr1_complex_bromodomain_subunit_Brf1	4×10 ⁻¹⁰⁶	78.8	8.4	5.9	3.3	0.34
G7K_6360-t1#	gi_19113748_ref_NP_592836.1_cell_wall_protein_Asl1_predicted_O-glucosyl_hydrolase	1×10 ⁻³³	358.1	147.5	108.3	79.8	0.91
G7K_6363-t1*#	gi_19075485_ref_NP_587985.1_20S_proteasome_component_beta_3_Pup3_(predicted)	1×10 ⁻¹⁰⁶	219.7	428.3	212.5	152.7	0.81
G7K_6381-t1	gi_19112124_ref_NP_595332.1_cysteine_synthase	6×10 ⁻¹⁵⁷	129.0	5.9	3.9	2.6	0.71
G7K_6516-t1*#	gi_19115488_ref_NP_594576.1_3-isopropylmalate_dehydratase_Leu2_(predicted)	0	188.8	104.7	64.5	41.4	0.46
G7K_6537-t1*#	no hit		2973.8	2751.4	1588.9	1109	0.71
G7K_6581-t1*#	gi_19113432_ref_NP_596640.1_dolichol-phosphate_mannosyltransferase_subunit_3	1×10 ⁻⁹	485.5	70.6	32	12.7	0.6
G7K_6602-t1*#	no hit		1031.0	347.2	222.7	165.8	0.85
G7K_6616-t1*	gi_429242792_ref_NP_594069.2_endocytosis_protein	0	95.5	137.2	87.6	65.2	0.67
G7K_6625-t1*#	gi_19114619_ref_NP_593707.1_acyl-coA-sterol_acyltransferase_Are1_(predicted)	8×10 ⁻¹²¹	84.0	227.8	134.6	100.2	0.68
G7K_6634-t1#	no hit		69.4	111.3	75.4	51.9	0.43
G7K_6654-t1#	gi_19113884_ref_NP_592972.1_saccharopine_dehydrogenase_Lys3	8×10 ⁻¹⁷⁹	148.8	267.6	184.2	130.4	0.76
G7K_6783-t1*#	gi_19113064_ref_NP_596272.1_pyruvate_dehydrogenase_e1_component_beta_subunit_Pdb1	1×10 ⁻¹⁷⁶	1018.6	371.4	235	151.5	0.79
G7K_6868-t1*#	no hit		119.7	2745.3	354.9	256.2	-0.23
G7K_6890-t2*#	gi_19075338_ref_NP_587838.1_nucleosome_assembly_protein_Nap1	4×10 ⁻¹²⁹	256.2	240.9	139	90	0.94

*Significantly ($p < 0.05$) differentially expressed genes between growths in 1 µg/mL and 2 µg/mL of TSA.

#Significantly ($p < 0.05$) differentially expressed genes between growths in 2 µg/mL and 3 µg/mL of TSA.

References

1. Igo-Kemenes T, Hörz W, Zachau HG (1982) Chromatin. *Ann Rev Biochem* 51: 89–121.
2. Luger K, Mäder AW, Richmond RK, et al. (1997) Crystal structure of the nucleosome core particle at 2.8 Å resolution. *Nature* 389: 251–260.
3. Millar CB, Grunstein M (2006) Genome-wide patterns of histone modifications in yeast. *Nat Rev Mol Cell Biol* 7: 657–666.
4. Li B, Carey M, Workman JL (2007) The role of chromatin during transcription. *Cell* 128: 707–719.
5. Luger K, Richmond TJ (1998) The histone tails of the nucleosome. *Curr Opin Genet Dev* 8: 140–146.
6. Sasaki K, Ito T, Nishino N, et al. (2009) Real-time imaging of histone H4 hyperacetylation in living cells. *Proc Natl Acad Sci USA* 106: 16257–16262.
7. Yoshida M, Horinouchi S, Beppu T (1995) Trichostatin A and trapoxin: novel chemical probes for the role of histone acetylation in chromatin structure and function. *BioEssays* 17: 423–430.
8. Nishida H, Motoyama T, Suzuki Y, et al. (2010) Genome-wide maps of mononucleosomes and dinucleosomes containing hyperacetylated histones of *Aspergillus fumigatus*. *PLOS ONE* 5: e9916.
9. Liu Y, Leigh JW, Brinkmann H, et al. (2009) Phylogenomic analyses support the monophyly of Taphrinomycotina, including *Schizosaccharomyces* fission yeasts. *Mol Biol Evol* 26: 27–34.
10. Nishida H, Sugiyama J (1994) Archiascomycetes: detection of a major new lineage within the Ascomycota. *Mycoscience* 35: 361–366.
11. Goto S, Sugiyama J, Hamamoto M, et al. (1987) *Saitoella*, a new anamorph genus in the Cryptococcaceae to accommodate two Himalayan yeast isolates formerly identified as *Rhodotorula glutinis*. *J Gen Appl Microbiol* 33: 75–85.
12. Nishida H, Hamamoto M, Sugiyama J (2011) Draft genome sequencing of the enigmatic yeast *Saitoella complicata*. *J Gen Appl Microbiol* 57: 243–246.
13. Nishida H, Matsumoto T, Kondo S, et al. (2014) The early diverging ascomycetous budding yeast *Saitoella complicata* has three histone deacetylases belonging to the Clr6, Hos2, and Rpd3 lineages. *J Gen Appl Microbiol* 60: 7–12.
14. Ekwall K, Olsson T, Tumer BM, et al. (1997) Transient inhibitor of histone deacetylation alters the structural and functional imprint at fission yeast centromeres. *Cell* 91: 1021–1032.
15. Yamauchi K, Kondo S, Hamamoto M, et al. (2015) Draft genome sequence of the archiascomycetous yeast *Saitoella complicata*. *Genome Announc* 3: e00220–15.
16. Trapnell C, Pachter L, Salzberg SL (2009) TopHat: discovering splice junctions with RNA-Seq. *Bioinformatics* 25: 1105–1111.
17. Li H, Handsaker B, Wysoker A, et al. (2009) The Sequence Alignment/Map format and SAMtools. *Bioinformatics* 25: 2078–2079.
18. Ogasawara O, Mashima J, Kodama Y, et al. (2013) DDBJ new system and service refactoring. *Nucleic Acids Res* 41: D25–D29.
19. Robinson MD, McCarthy DJ, Smyth GK (2010) edgeR: a Bioconductor package for different expression analysis of digital gene expression data. *Bioinformatics* 26: 139–140.
20. Valouev A, Johnson SM, Boyd SD, et al. (2011) Determinants of nucleosome organization in

- primary human cells. *Nature* 474: 516–520.
21. Kaplan N, Moore IK, Fondufe-Mittendorf Y, et al. (2008) The DNA-encoded nucleosome organization of a eukaryotic genome. *Nature* 458: 362–366.
 22. Altschul SF, Gish W, Miller W, et al. (1990) Basic local alignment search tool. *J Mol Biol* 215: 403–410.
 23. Amit M, Donyo M, Hollander D, et al. (2012) Differential GC content between exons and introns establishes distinct strategies of splice-site recognition. *Cell Rep* 1: 543–556.
 24. Nishida H, Katayama T, Suzuki Y, et al. (2013) Base composition and nucleosome density in exonic and intronic regions in genes of the filamentous ascomycetes *Aspergillus nidulans* and *Aspergillus oryzae*. *Gene* 525: 5–10.
 25. Yu J, Hu S, Wang J, et al. (2002) A draft sequence of the rice genome (*Oryza sativa* L. ssp. *indica*). *Science* 296: 79–92.
 26. Nishida H, Kondo S, Matsumoto T, et al. (2012) Characteristics of nucleosomes and linker DNA regions on the genome of the basidiomycete *Mixia osmundae* revealed by mono- and dinucleosome mapping. *Open Biol* 2: 120043.
 27. Graessle S, Dangl M, Haas H, et al. (2000) Characterization of two putative histone deacetylase genes from *Aspergillus nidulans*. *Biochim Biophys Acta* 1492: 120–126.
 28. Andersson R, Enroth S, Rada-Iglesias A, et al. (2009) Nucleosomes are well positioned in exons and carry characteristic histone modifications. *Genome Res* 19: 1732–1741.
 29. Chen W, Luo L, Zhang L (2010) The organization of nucleosomes around splice sites. *Nucleic Acids Res* 38: 2788–2798.
 30. Schwartz S, Ast G (2010) Chromatin density and splicing density: on the cross-talk between chromatin structure and splicing. *EMBO J* 29: 1629–1636.
 31. Schwartz S, Meshorer E, Ast G (2009) Chromatin organization marks exon–intron structure. *Nat Struct Mol Biol* 16: 990–995.
 32. Tilgner H, Nikolaou C, Althammer S, et al. (2009) Nucleosome positioning as a determinant of exon recognition. *Nat Struct Mol Biol* 16: 996–1001.
 33. Tsankov A, Yanagisawa Y, Rhind N, et al. (2011) Evolutionary divergence of intrinsic and trans-regulated nucleosome positioning sequences reveals plastic rules for chromatin organization. *Genome Res* 21: 1851–1862.
 34. Shim YS, Choi Y, Kang K, et al. (2012) Hrp3 controls nucleosome positioning to suppress non-coding transcription in eu- and heterochromatin. *EMBO J* 31: 4375–4387.



AIMS Press

© 2016 Hiromi Nishida, et al., licensee AIMS Press. This is an open access article distributed under the terms of the Creative Commons Attribution License (<http://creativecommons.org/licenses/by/4.0>)